

Electron trapping mechanisms injection guns

Cite as: Phys. Plasmas 23, 013105 (2016) / doi.org/10.1063/1.4941705
Submitted: 26 October 2015 • Accepted: 28 January 2016

Ioannis Gr, Berghoef, J.P. Slob, & Z. Zetianogl.



View Online



Export Citation



CrossMark

ARTICLES YOU MAY BE INTERESTED IN

Triode magnetron injection gun for the KIT 2 MW 1 Physics of Plasmas 23, 013105 (2016) / doi.org/10.1063/1.4941705

Magnetic field profile analysis for gyrotron experiments Physics of Plasmas 24, 037122 (2017) / doi.org/10.1063/1.4977100

Influence of emitter ring manufacturing tolerance on gyrotrons Physics of Plasmas 23, 083103 (2016) / doi.org/10.1063/1.4959000

Physics of Plasmas 23, 013105 (2016) / doi.org/10.1063/1.4941705



Physics of Plasmas

Features in Plasma Physics Webinars

Submit Today!

Electron trapping mechanisms in magnetron injection guns

Ioannis Gr. Pagonakis,^{1,a)} Bernhard Piosczyk,¹ Jianhua Zhang,¹ Stefan Illy,¹ Tomasz Rzesnicki,¹ Jean-Philippe Hogge,² Konstantinos Avramidis,¹ Gerd Ganzenbein,¹ Manfred Thumm,¹ and John Jelonnek¹

¹Karlsruhe Institute of Technology (KIT), IHM, 76131 Karlsruhe, Germany

²École Polytechnique Fédérale de Lausanne, Swiss Plasma Center (SPC), 1015 Lausanne, Switzerland

(Received 26 October 2015; accepted 28 January 2016; published online 11 February 2016)

A key parameter for the gyrotron operation and efficiency is the presence of trapped electrons. Two electron trapping mechanisms can take place in gyrotrons: (i) the adiabatic trap and (ii) the magnetic potential well. Their influence on the gyrotron operation is analyzed. Two gun design criteria are then proposed to suppress both mechanisms in order to minimize the risk of possible problems. Experimental results of three high power gyrotrons are presented and their performance is correlated to the presence of populations of trapped electrons. Finally, some very general gun design principles are presented for the limitation of harmful electron trapping.

[<http://dx.doi.org/10.1063/1.4941705>]

I. INTRODUCTION

The gyrotron is a millimeter and submillimeter wave source device which is extensively used for plasma heating and current drive applications. The gyrotron operation is based on the electron cyclotron resonance maser (CRM) instability. The transverse energy of the electron gyro-motion is converted to an electromagnetic wave in a cylindrical open cavity. The electrons form a hollow electron beam (HEB) and are guided by an externally applied static magnetic field that determines the source frequency. The beam quality at the entrance of the cavity plays an important role on the interaction efficiency η_e which ranges typically between 20% and 40%. A magnetron injection gun (MIG) is used for the generation of the electron beam. The geometry of the MIG subcomponents determines the quality of the HEB at the cavity. The beam electrons are produced by thermionic emission of a heated emitter ring, which is part of the cathode, the main subcomponent of the MIG. The electrons are accelerated by the voltage U_a applied between the cathode and a second electrode, the anode. The convergent externally applied magnetic field guides the electrons towards the cavity and generates the required gyro-motion of the beam electrons.

For the design and the study of MIGs, electron optics codes have been developed, such as *Ariadne*,¹ *ESRAY/ESPIC*,² *DAPHNE*,³ *EGUN*,⁴ and *EPOSR*. In practice, the operation of the gun is not as ideal as it is in the numerical simulations. The gyrotron operation can be influenced by many factors that are not usually taken into account during the design phase of the MIG. Such a factor is the presence of trapped electrons which can dramatically influence the gyrotron operation.^{5–7}

In this paper, two electron trapping mechanisms in gyrotrons are discussed. Based on the theoretical and experimental results, two MIG design criteria are proposed for the suppression of trapped electrons in a MIG. Experimental results of three high power gyrotrons are presented with

relevance to the design criteria. Finally, some general design principles for a MIG are presented, in order to fulfill the proposed design criteria.

II. ADIABATIC TRAP

The beam parameters at the cavity determine the interaction efficiency and the generated microwave power. The main parameters of the HEB are as follows: (i) The beam radius r_b which should be close to the radius of the first maximum of the nominal TE mode for an efficient interaction. (ii) The beam thickness Δr_b which should remain smaller than one fifth of the wavelength ($\lambda/5$) of the generated RF power.⁸ (iii) The beam power P_b before the interaction, i.e., the product of the beam current I_b and the beam voltage U_b , which represents the potential energy eU_b transformed to kinetic energy during the acceleration of the beam from the cathode towards the cavity entrance. Here, e is the electron charge. The difference $U_a - U_b$ is known as voltage depression and it is related to the level of the neutralization at the cavity.⁹ (iv) The pitch factor α which is defined as the ratio $\alpha = v_{\perp}/v_{\parallel}$, where v_{\perp} and v_{\parallel} are the transverse and the parallel components of the velocity, with respect to the magnetic field, determines the fraction of transverse energy of the electrons' gyro-motion. This parameter is very important due to the fact that only the transverse energy of the electrons interacts with the RF mode at the cavity and consequently the interaction efficiency η_e is limited by $\eta_e < \alpha^2/(1 + \alpha^2)$. (v) Finally, the transverse velocity spread δv_{\perp} , defined as the root-mean-square of the transverse velocity distribution, which should ideally be as low as possible.

Typical values for the mean pitch angle in high power gyrotrons range between 1.2 and 1.4. The design of gyrotrons with a higher pitch factor is not common, despite the increase of the interaction efficiency, in order to limit the influence of the harmful adiabatically trapped electrons. The adiabatic trap is a well known electron trapping mechanism in gyrotrons. It takes place in the region between the cathode and the cavity where the magnetic field lines converge. The transverse velocity of the beam electrons is increasing due to

^{a)}E-mail: ioannis.pagonakis@kit.edu

the conservation of the adiabatic invariant $\gamma^2 v_{\perp}^2/B$,¹⁰ whereas the parallel velocity v_{\parallel} decreases in such a way that the total energy is conserved (γ is the relativistic factor). As a result, some electrons can be reflected back by magnetic mirroring towards the cathode depending on their initial transverse velocity. On the other side, the decelerating field of the cathode reflects the electrons towards the cavity (electric mirror).

It has been experimentally shown¹¹ that even for average pitch factors less than one, a population of adiabatically trapped electrons was observed. The velocity spread could be much higher than the expected one due to many uncontrolled factors such as roughness of the emitting surface, manufacturing tolerances, and misalignments. Therefore, a small population of the beam electrons could have initial conditions which cause them to be adiabatically trapped, leading to the formation of a halo around the main beam. Several theoretical and experimental studies have been published mainly by Russian scientists^{11–14} on the study of the adiabatically trapped electrons. Electrons can escape from the trap by two different ways. During the oscillations in the trap, the values of the adiabatic invariant may be affected by the high electric fields in the acceleration region which perturb the adiabaticity. Then, it is possible that electrons overcome the magnetic mirror and escape through the cavity. On the other hand, the total energy of the trapped electrons could also be perturbed due to the resonant periodic forces which are caused by the longitudinal oscillations of the space charge in the trapping region.¹⁵ Then, a portion of the trapped electrons could overcome the electric mirror and reach the cathode surface with energy up to the order of few keV.

The secondary electrons emitted from the bombarded area of the cathode surface play a critical role in the accumulation of particles in the trap and in the formation of the beam halo. It is remarkable that the secondary emission yield for molybdenum, which is commonly used for the cathode subcomponents on both sides of the emitter ring, could be greater than 2 for incident angles higher than 60° .¹⁷ The importance of the secondary electrons on the accumulation of trapped charge in a low power and low frequency gyrotron was demonstrated using time consuming PIC simulations.¹² In that work, the bombarded area on the cathode surface was extended from the middle of the emitter ring towards the rear part of the gun by about three times the length of the emitter ring thickness. The time required for the stabilization of the beam halo was of the order of several tens of nanoseconds.

During the experiments with the first industrial prototype of the EU 170 GHz/2 MW/CW coaxial cavity gyrotron for ITER,⁶ several instabilities were observed which are attributed to the influence of the secondary electrons emitted from the cathode surface. In particular, voltage standoff instabilities and leakage currents on the body and the coaxial insert limited the operation of the gyrotron in voltages less than 85 kV when the nominal voltage was 90 kV. Electron traces at many positions on the surface of the gyrotron components were observed during the inspection of the tube after the end of the experiments. A correlation of the positions of most of the damaged spots with trapped electrons has been

found by numerical simulations.²³ It is remarkable that three of these were found on parts of the gyrotron surface that are intersected by magnetic field lines which guide adiabatically trapped electrons emitted from the cathode surface. In particular, a damage at the end of the launcher could be correlated with the adiabatically trapped electron emitted from the rear part of the gun (region A in Fig. 1), while a damage on the coaxial insert and many electron traces on the cathode nose could be correlated with the adiabatically trapped electrons emitted from the cathode nose (region B in Fig. 1). Based on these observations, the hypothesis that the beam halo is generated in the magnetic field lines which guide adiabatically trapped electrons emitted from the cathode surface was considered.

Recently, this hypothesis was validated by time-consuming PIC simulations of the first industrial prototype using the ESPIC code.² The code ESPIC is an extension of the electrostatic code ESRAY, which can simulate slowly varying effects in the gyrotron electron gun. The classical PIC approach is used for the particle handling, while for the calculation of the electric fields in two dimensions a multi-grid Poisson-solver is used. In Fig. 2, the evolution of the beam halo is presented for several times ranging from 0 to 4 μ s. At 0.05 μ s, the beam halo surrounds only the main beam while at 1 μ s a small population of trapped electrons bombards the region A of the cathode surface. Due to the fact that the secondary electrons emitted from the region A are adiabatically trapped, at 2 μ s, a beam halo with a significant number of trapped electrons is generated. The space charge of the beam halo supported by the region A strongly influences the beam parameters: (i) decreases the pitch factor of the electrons emitted from the emitter ring and (ii) decreases also the beam current due to the fact that Schottky effect is taken into account in the simulations. In addition, the pitch factor of the electrons emitted from the region between the emitter ring and the region A is also decreasing influencing the halo generation from that area. Later on, a small number of trapped electrons also bombards the region B of the cathode surface and at 4 μ s accumulation begins. Then, a secondary halo beam is generated along the magnetic field lines intersecting the B region of the cathode surface.

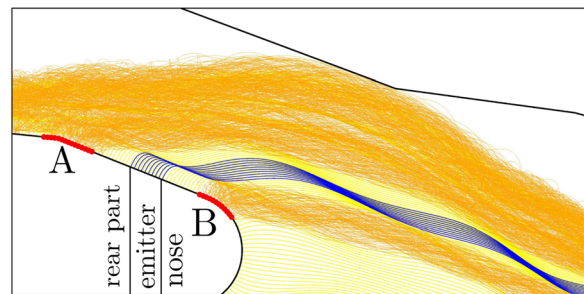


FIG. 1. Trajectories of the electrons emitted from the cathode surface of the MIG of the EU 170 GHz/2 MW/CW coaxial cavity gyrotron for ITER with zero initial velocity. The main beam is plotted in blue, the adiabatically trapped electron trajectories are in orange while in yellow the trajectories of the non-trapped electrons emitted from the cathode surface. The area of the cathode surface from which adiabatically trapped electrons are emitted is noted in red.

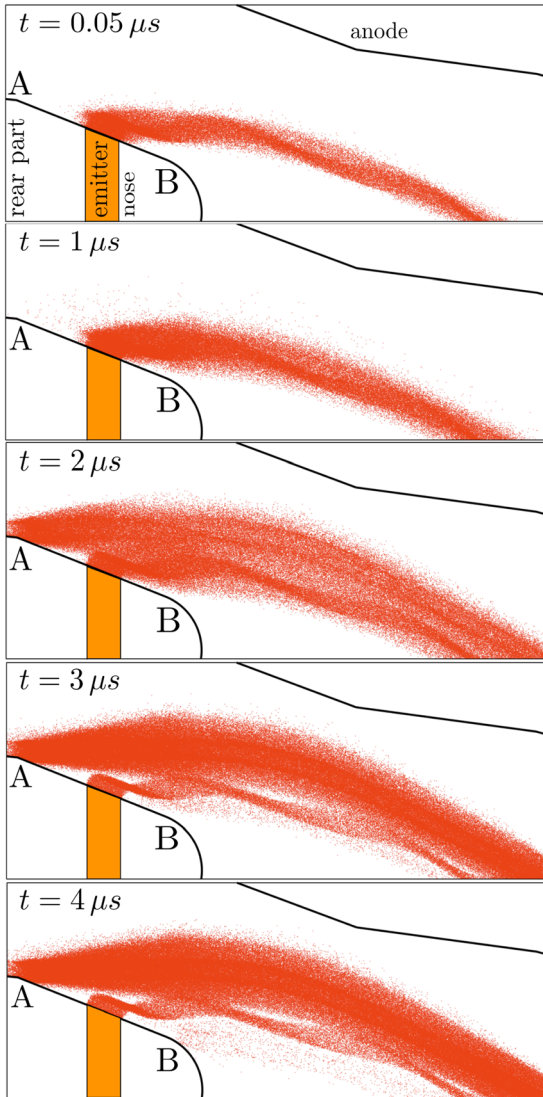


FIG. 2. Evolution of the trapped electron accumulation in the MIG of the EU 170 GHz/2 MW/CW coaxial cavity gyrotron for ITER.

The generation of the inner beam halo around the region B is caused by the small fraction of the secondary electrons emitted from the cathode surface between the beam and the region B which can also be trapped due to fact that the initial velocity of the secondary electrons is not zero. This population of trapped secondary electrons cannot generate a significant beam halo but it is enough to extend the beam halo from the emitter ring to the region B, where the majority of the secondary electrons emitted are adiabatically trapped. The diffusion of the secondary electron emission along cathode surface takes place due to the fact that the magnetic field line followed by a secondary electron is different from the magnetic field line guiding the incident electron. This is because (i) the intersecting point of the incident electron trajectory on the cathode surface, in general, is different from the point where the magnetic field line intersects the cathode surface (Larmor radius is not necessarily zero) and (ii) the initial velocity of the secondary electron. This way, the emission of secondary electrons gradually extends to a larger area of the cathode surface, reaching finally the region B. The characteristic time evolution of this process is slower than

the generation of the beam halo in region A. In the reality, that phenomenon is expected earlier than the simulation predicts due to the fact that the number of the electrons in simulations is significantly less than in the reality and the probability of some electrons to reach the region B causing ignition of the beam halo is much higher.

The accumulation of trapped electrons in the inner beam halo is expected to continue further after $4\ \mu s$. The simulation of this gun was not extended to longer times due to practical reasons related to the required computation time. The calculation time of the halo evolution in the first $4\ \mu s$ required about a week on a 4 cores shared memory parallel computer system at KIT. It should be noted that an emitter surface roughness of the order of $50\ \mu m$ is considered while for the generation of the secondary electrons, a modified emission model presented in Ref. 16 was used. The maximum value of the secondary emission coefficient for Mo with a value of 1.9 under perpendicular bombardment of the primary electron was also considered. The applied voltage was considered constant during the simulation. In order to limit the total number of particles in the simulation, 80 particles were emitted every 5 time steps, which in comparison with the cyclotron period at the cavity is 0.085. The typical number of macro-electrons at a time moment is of the order of 2.5×10^5 . More details on that work will be presented in the scientific community soon in a dedicated publication. The main conclusion of these preliminary PIC simulation is that the beam halo has the tendency to be generated along the magnetic field lines which intersect the cathode surface in the regions where the probability of adiabatically trapped secondary electrons is high.

Based on the above analysis and the experimental results, a gun design criterion is proposed in order to suppress the generation of a harmful beam halo. In particular, the design of the cathode should minimize the number of secondary electrons emitted from the cathode surface which are adiabatically trapped.

In practice, only a limited part of the cathode surface in the vicinity of the emitter ring is usually critical for possible emission of adiabatically trapped electrons. Electrons emitted from this area are guided by the magnetic field lines toward the compression region between the cathode and the cavity whereas electrons emitted from all other parts of the cathode surface are either guided to the anode or to the coaxial insert (for the coaxial cavity gyrotron) or to an insulation ceramic at the rear part of the MIG. It is also possible for electrons emitted from some cathode areas to be trapped due to the existence of a potential well, the second trapping mechanism in gyrotrons. This will be discussed in Section III.

The necessary calculations in order to check whether the proposed design criterion is satisfied or not are performed very quickly. A self-consistent, electrostatic, trajectory code such as Ariadne could be used for this purpose. Therefore, this criterion could be easily applied during the design phase of a MIG, in which many geometries are checked, and PIC simulations cannot be used due to excessive computation time.

The trajectories of sample secondary electrons emitted from the critical area of the cathode surface are calculated in order to ensure that they are not trapped. The initial kinetic energies E_0 of the secondary electrons are given by the typical probability density function (PDF)¹⁸ of the true secondary electrons emitted from a molybdenum surface bombarded by electrons with energy more than few tens of electron-volts shown at the top of Fig. 3. The initial kinetic energy of the majority of true-secondary electrons is less than 50 eV. On the other hand, the true-secondary electrons have a $\sim \cos(\theta)$ distribution in angle, which is fairly independent of the primary incident angle θ_0 and the incident energy.¹⁹

In practice, the adiabatic invariant value of the secondary electrons is mostly determined by the azimuthal component of their initial velocity. Based on the initial energy and the angular distributions, the PDF and the cumulative distribution function (CDF) of the initial energy $E_{0\phi}$ on the azimuthal direction have been generated as shown at the bottom of Fig. 3. The sign represents the direction of the azimuthal component of the initial velocity relative to the vector $\mathbf{v}_0 = \mathbf{E} \times \mathbf{B}/B^2$. It is concluded that for 95% of the secondary electrons is $E_{0\phi} < 5$ eV and for 99% $E_{0\phi} < 10$ eV.

An even simpler definition of the design criterion could be given based on the adiabatic approximation. The dimensionless transverse (i.e., perpendicular to the magnetic field)

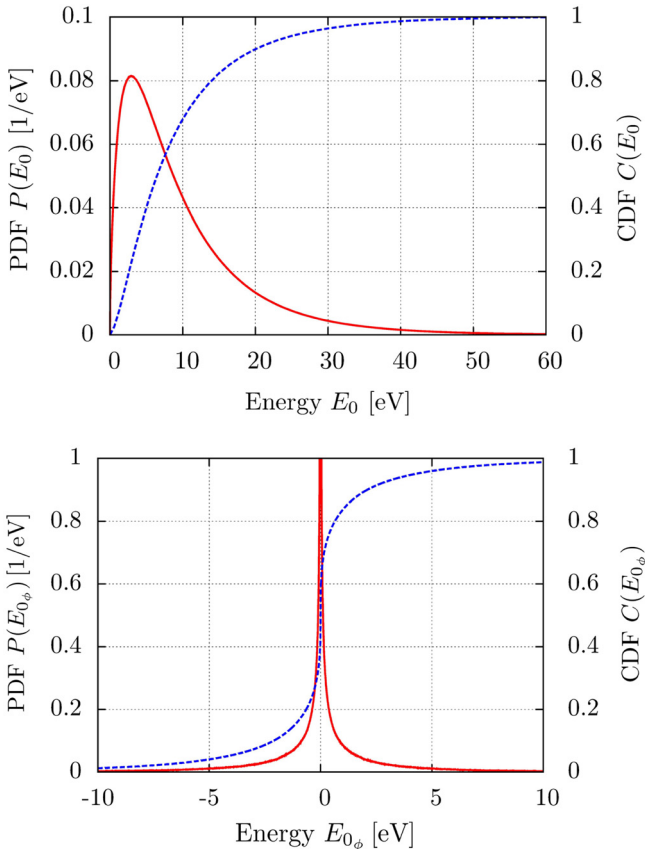


FIG. 3. The typical probability density function (solid curve) and the cumulative distribution function (dashed curve) versus the total initial kinetic energy (at the top) and the initial kinetic energy on the azimuthal direction (at the bottom) of the secondary electrons emitted from a molybdenum surface bombarded by electrons of energy higher than few eVs.

momentum $u_{r\perp}$ at the cavity (or resonator) of the electrons emitted from the critical area of the cathode surface can be written as $u_{r\perp}^2 \approx (B_r/B_c) u_{c\perp}^2 = \kappa u_{c\perp}^2$, where $u_{c\perp}$ is the initial value. The ratio of the magnetic fields at the cavity B_r and the cathode B_c defines the magnetic compression κ . Due to the fact that B_c usually does not vary dramatically in the critical part of the cathode surface, the same compression $\kappa \approx \kappa_b = (r_e/r_b)^2$ is considered for all electrons emitted from the critical area. The constant κ_b is the compression of the electron beam which is a basic design parameter of the gyrotron.

A relation for the pitch factor α at the cavity of an individual electron emitted from the critical area with azimuthal component $u_{c\perp}$ of the initial dimensional momentum can be written as

$$\frac{\alpha^2}{\alpha^2 + 1} = \kappa_b \frac{u_{c\perp}^2}{\gamma_r^2 - 1}, \quad (1)$$

using the pitch factor definition $\alpha = v_{r\perp}/v_{r\parallel} = u_{r\perp}/u_{r\parallel}$, and the equation $\gamma_r^2 = 1 + u_{r\perp}^2 + u_{r\parallel}^2$, which correlates the relativistic factor γ_r at the cavity with the perpendicular $u_{r\perp}$ and the parallel $u_{r\parallel}$ components of the dimensionless momentum at the cavity. For an electron emitted with zero initial energy is¹⁰ $u_{c\perp} = u_{c0\perp} = E \times B/cB^2$, and Eq. (1) can be written as

$$\frac{\alpha_0^2}{\alpha_0^2 + 1} = \kappa_b \frac{u_{c0\perp}^2}{\gamma_r^2 - 1}, \quad (2)$$

where α_0 is the pitch factor at the cavity of a secondary electron emitted with zero initial kinetic energy. The azimuthal component of the transverse momentum can be written as $u_{c\perp} = u_{c0\perp} + u_{c1\perp}$, where

$$u_{c1\perp} = \sqrt{\gamma_0^2 - 1} = \sqrt{(1 + E_{0\phi}/mc^2)^2 - 1},$$

and where c and m are the speed of light in vacuum and the electron rest mass, respectively. It should be noted that the radial and axial components of the transverse initial momentum are neglected as was discussed above. Then, the pitch factor at the cavity of an electron emitted from the critical area of the cathode surface with an initial kinetic energy $E_{0\phi}$ in the azimuthal direction can be written as

$$\alpha(E_{0\phi}) = \frac{(\alpha_0 + \beta(E_{0\phi}) \sqrt{\alpha_0^2 + 1})}{\sqrt{\alpha_0^2 + 1 - (\alpha_0 + \beta(E_{0\phi}) \sqrt{\alpha_0^2 + 1})^2}}, \quad (3)$$

where the dimensionless function β is given by

$$\beta(E_{0\phi}) = \sqrt{\kappa_b \frac{(1 + E_{0\phi}/mc^2)^2 - 1}{\gamma_r^2 - 1}} \approx \sqrt{\kappa_b \frac{E_{0\phi}}{eU_a}}, \quad (4)$$

where $E_{0\phi} \ll eU_a$ in which the voltage depression has been neglected.

In Fig. 4, a comparison of the simulated and the approximated results based on Eq. (3) is shown for secondary electrons initial kinetic energies $E_{0\phi}$ of 20 and 50 eV. The results

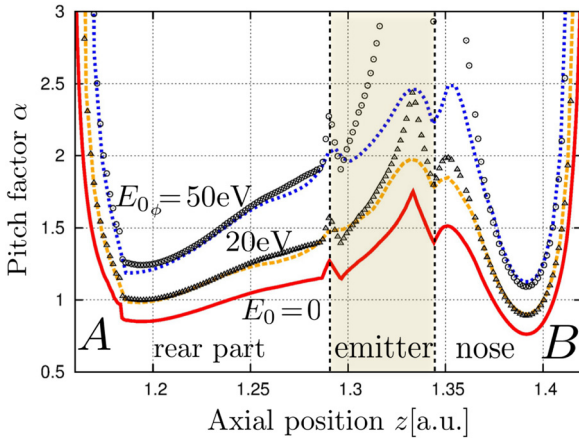


FIG. 4. Pitch factor at the cavity of the electrons emitted from the cathode surface with initial energies $E_{0\phi} = 0, 20$, and 50 eV as calculated by the self-consistent, trajectory code Ariadne (lines) and by Eq. (3) (points) for the nominal operating point of the first industrial prototype of the EU 170 GHz/ 2 MW coaxial cavity gyrotron project for ITER.

are in very good agreement for all initial positions, except for the emitter region where the space charge of the beam significantly influences the adiabaticity of the secondary electrons' trajectories.

Finally, meeting the newly defined criterion that no secondary electron emitted from the cathode surface is adiabatically trapped is equivalent to ensure that their pitch factor α at the cavity, given by Eq. (3), has a finite value. This is achieved if the pitch factor α_0 is lower than a threshold $\alpha_{\max}(E_{0\phi})$, in order to avoid an infinite value at the right hand side of Eq. (3), and it is given by the equation

$$\alpha_{\max}(E_{0\phi}) = \frac{1 - \beta(E_{0\phi})}{\sqrt{\beta(E_{0\phi})(2 - \beta(E_{0\phi}))}}. \quad (5)$$

Taking into account that the vast majority of the secondary electrons have initial azimuthal energy less than 10 eV, the maximal pitch factor α_{\max} at the cavity can be estimated for the secondary electrons emitted from the cathode. This value depends only on the magnetic compression κ_b and the accelerating voltage U_a . Therefore, the value of α_{\max} can be considered as a characteristic value for a gyrotron operating point. The variation of α_{\max} versus the magnetic compression κ_b for several values of the accelerating voltage is presented in Fig. 5. It should be pointed out that the pitch factor α_{\max} decreases significantly for magnetic compression larger than 10 .

In order to diagnose whether a MIG fulfills the design criterion or not, a special subroutine has been developed in the Ariadne code. The trajectories of sample electrons emitted from the critical area of the cathode with zero initial velocity are calculated, and the emitting points of the electrons which are adiabatically trapped or their pitch factor is greater or equal to α_{\max} are identified.

III. MAGNETIC POTENTIAL WELL

The second type of electron trapping in gyrotrons, also known as Penning mechanism, can take place wherever a magnetic field line intersects the equipotential lines as shown

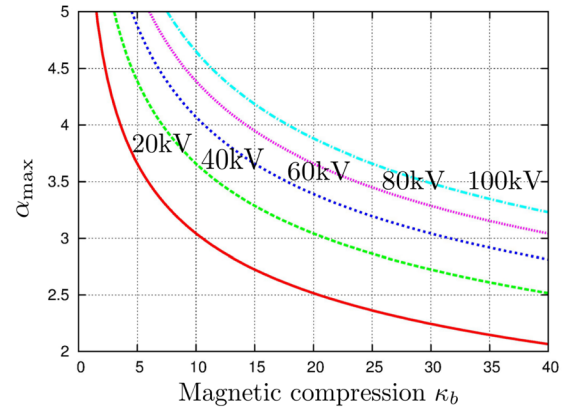


FIG. 5. Pitch factor α_{\max} versus the magnetic compression κ_b for several values of the accelerating voltage U_a and initial energy $E_{0\phi} = 10$ eV.

in Fig. 6. The electrons guided by the magnetic field line are accelerated from one side and decelerated from the other side by a force $F = -eE_{||}$ along the magnetic field line, where $E_{||}$ is the component of the electric field parallel to the magnetic field. A typical shape of the potential variation along the magnetic field line is shown in Fig. 7. The local maximum U_{\max} is the center of the potential well. The depth and the size of the potential well are determined by the highest U_{\min} on both sides along the magnetic field line from the center of the well. The maximum depth of the potential well is $U_d = U_{\max} - U_{\min}$. The trapped electrons which have an energy lower than eU_d , oscillate around the center of the potential well. The transverse component of the electric field E_{\perp} causes an azimuthal drift $v_d = E \times B / B^2$ to the electrons and therefore a rotation around the gyrotron axis of symmetry.

Such a potential well is inherently created in the gyrotron operation with a depressed collector between the cathode and the decelerating region of the collector. All electrons with an energy below the retarding collector potential are reflected back to the cathode. This results in trapping since the cathode retarding potential is significantly higher than the collector potential. Thus, the spent beam electrons with the lowest energy mainly contribute to the accumulation of the trapped electron depending on the retarding collector voltage. No problems are foreseen for decelerating voltage when only a small population of the beam electrons are reflected. In these cases, it has been shown^{20,21} that the trapped electrons gain energy passing through the cavity and

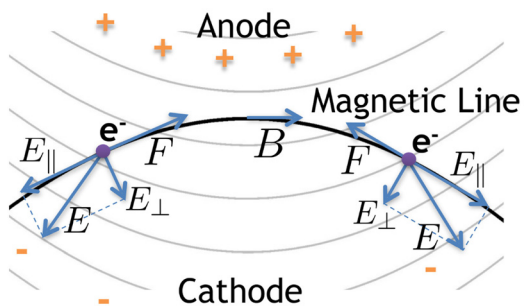


FIG. 6. The equipotential lines are intersected by a magnetic field line formulating a magnetic potential well.

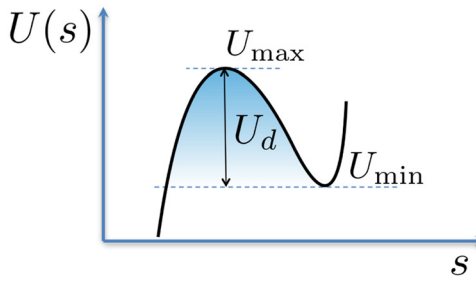


FIG. 7. The magnetic potential well definition is based on the variation of the potential along a magnetic field line.

they first overcome the electrostatic barrier of the collector since the barrier towards the cathode is significantly higher (by typically 20 keV). A further mechanism which allows the trapped electrons to leave the trap is radial diffusion towards the walls. The diffusion rate depends on the geometry (radial distance) of the walls surrounding the beam.

A magnetic potential well is not always harmless. A potential well in the MIG region could have a strong detrimental influence on the gyrotron operation.^{5,6} The trapped electrons population increases gradually due to the ionization of the residual gas inside the gyrotron. Discharges could take place when the space charge in the well reaches a critical value. The characteristic evolution time of the discharges depends mainly on the pressure in the tube. This can be shown using a simple model in which it is supposed that the potential well causes harmonic oscillations on the trapped electrons. The potential along the magnetic field can be approximated at lowest order by $U(x) = -ax^2$, where $a > 0$ in V/m². The trapped electrons in this potential well oscillate with a velocity given by

$$v(t) = \sqrt{\frac{2eU_0}{m}} \sin(\omega t), \quad (6)$$

where the bouncing frequency is given by $\omega = \sqrt{2ea/m}$. The number of ionizations N_T during a period T_e of the electron bounce is given by $N_T = V_e n_b$, where V_e is the effective volume which the electron covers during a period and n_b is the background gas density. V_e is calculated by the integral

$$V_e = \int_0^{T_e} \sigma(E_k) v(t) dt \quad (7)$$

or

$$V_e = \frac{T_e}{2\pi} \sqrt{\frac{2eU_0}{m}} \int_0^{2\pi} \sigma(U_0 \sin^2(\phi)) \sin(\phi) d\phi, \quad (8)$$

where σ represents the cross section of the ionization collision of the electrons with the molecules of the residual gas. It is a known function of electron kinetic energy and it depends on the type of molecules of the gas in the tube. On the other hand, the background gas density is estimated using the ideal gas equation

$$n_b = \frac{N_A}{RT} P, \quad (9)$$

where N_A is the Avogadro number, R is the universal gas constant, T is the temperature, and P is the pressure inside the tube.

The average time τ_i between two ionizations is given by the following equation:

$$\tau_i = \frac{T_e}{V_e n_b}, \quad (10)$$

while the product of τ_i with the pressure P is

$$\tau_i \cdot P = 2\pi \sqrt{\frac{m}{2eU_0} \frac{RT}{N_A}} \frac{1}{\int_0^{2\pi} \sigma(U_0 \sin^2(\phi)) \sin(\phi) d\phi}. \quad (11)$$

In Fig. 8, the variation of the product $\tau_i \cdot P$ is presented as a function of the total energy of the trapped electrons eU_0 , considering that the residual gas in the gyrotron consists only of nitrogen²² at room temperature ($T = 300$ K). The minimum value of this product is 0.3×10^{-6} ms·mbar at the energy of 1.5 keV, while it does not vary significantly with the total energy of the trapped electrons for $E_0 > 0.2$ keV.

Assuming that during the accumulation process no electrons escape out of the trap, then the ionization of the background molecules by the trapped electrons results in an avalanche type increase (due to doubling the number per step) of the trapped electrons. Thus, the number of trapped electrons increases with time approximately as $n_e(t) \approx n_{e_0} \cdot 2^{t/\tau_i}$, where n_{e_0} is the number of electrons in the trap at the beginning of the pulse. Then the rate of accumulation of the charge is defined as

$$i_t(t) = e dn_e(t)/dt = e n_{e_0} \ln(2) \frac{2^{t/\tau_i}}{\tau_i}.$$

The required time τ_a to reach a significant rate of electron accumulation in a trap of the order of $i_t \approx 100$ mA for several values of the pressure is estimated (considering $n_{e_0} = 1$ and $\tau_i \cdot P = 0.3 \cdot 10^{-6}$ ms · mbar) and it is presented in Table I.

The pressure in a gyrotron usually ranges between 10^{-6} and 10^{-8} mbar and therefore the influence of the potential well in gyrotrons is expected for times above 10 ms.

The existence of potential wells in gyrotrons may decrease significantly the high voltage performance. The

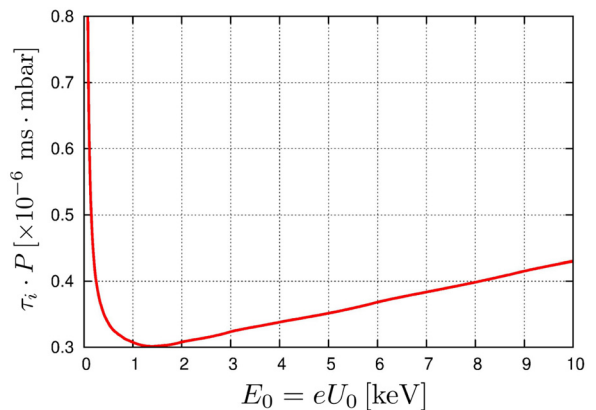


FIG. 8. The product of the average ionization time and the pressure versus the total energy of the trapped electron.

TABLE I. Accumulation time versus pressure.

Pressure P (mbar)	Accumulation time τ_a
10^{-4}	0.15 ms
10^{-6}	17.3 ms
10^{-8}	1.94 s
10^{-10}	3.6 min

existence of such a harmful potential well can be experimentally observed by applying a gradually increasing voltage to the electron gun in the presence of the magnetic field, with a cold emitter. Usually, a periodic or constant leakage current is measured which is much higher than the expected field emission current. This current is the result of discharges of the trapped electrons from the potential well.

The prognosis whether a potential well is harmful or not is not an easy task. A more comprehensive work is needed in order to analyze the influence of the shape, depth, and pressure on the voltage stand-off stability and to ensure that a potential well is not going to create problems. In order to minimize the risk, the formation of any potential well in the gyrotron should be avoided by an appropriate design of MIG electrodes.

A dedicated subroutine has been incorporated in the Ariadne code facilities in order to identify automatically the regions of magnetic potential well traps. The code calculates the electrostatic potential $U(s)$ along each magnetic field line in the MIG region separately. For each local maximum U_{\max} , the two minimum potentials on both sides of the local maximum are calculated. The higher one of the two minima U_{\min} determines the depth of the well along the magnetic field line which is defined as $U_d(s) = U(s) - U_{\min}$.

IV. EXPERIMENTAL RESULTS

The unstable behaviour observed in the experiments of the first industrial prototype of the EU 170 GHz/2 MW coaxial cavity gyrotron project for ITER was attributed to the two trapping mechanisms described above. Voltage stand-off problems even with cold emitter were observed in the presence of the nominal magnetic field in the experiments with a high impedance power supply. Periodic discharges were observed for voltages around 60 kV, while for voltages more than 63 kV the leakage current exceeded the power supply current limitation. During short-pulse experiments with the electron beam, strong instabilities limited the operation of the gyrotron for accelerating voltages higher than 80–82 kV, although the nominal voltage is 90 kV.

In the region of the MIG, both types of electron trapping mechanisms coexist, as shown in Fig. 9. A magnetic potential well is formed at the rear part of the cathode with a maximum depth of about 35 kV. It extends from the outer cathode surface to the corona ring of the anode. The cathode outline is subdivided into four domains according to the different behavior of the electrons emitted from each. The domain between the points 2 and 3 is the critical one concerning the adiabatic trap. Electrons emitted from this part of the cathode are guided by the magnetic field towards the cavity. The

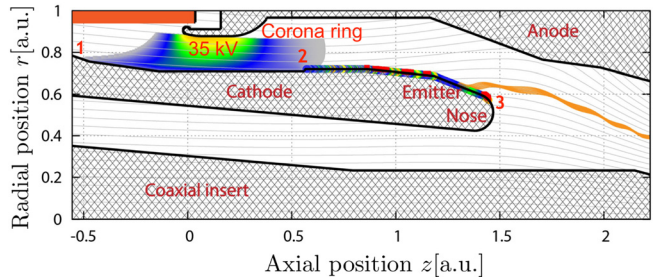


FIG. 9. Electron trappings in the first industrial prototype of the EU 170 GHz/2 MW coaxial cavity gyrotron project for ITER.

varyations of the pitch factor at the cavity is indicated by different colors on the emitting point along the outline of the cathode. The emitting points of the adiabatically trapped electrons are plotted in red. In addition, the pitch factor at the cavity as a function of the axial position of the emitting points is shown in Fig. 10. Electrons emitted from the domain indicated by the points 1 and 2 remain trapped due to the magnetic potential well. The trajectories of the electrons emitted from the left of the point 1 intersect the anode after passing through the potential well. On the other hand, electrons emitted from the inner side of the cathode and the nose below point 3 are collected by the coaxial insert.

For the design of the MIG of the refurbished first industrial prototype for the EU coaxial cavity gyrotron project for ITER,²³ the electron trapping mechanisms suppression criteria have been partly considered. As shown in Figs. 11 and 12, the potential well and the adiabatically trapped electrons emitted from the cathode surface were eliminated. However, the pitch factor of the electrons emitted from the rear part is $\alpha_0 = 7.5$, significantly higher than the safe value $\alpha_{\max} \approx 3$ given by Eq. (5) taking into account the nominal accelerating voltage $U_a = 90$ kV and the magnetic compression $\kappa_b \approx 35$. The voltage stand-off stability of the new gun was checked before the delivery of the industrial tube with a mock-up device without emitter ring.²⁴ It is remarkable that the voltage stand-off in these tests was excellent even in poor vacuum conditions. The pressure in the mock-up device was estimated to be of the order of 10^{-3} mbar while in the gyrotrons the pressure is expected to be at least three orders of

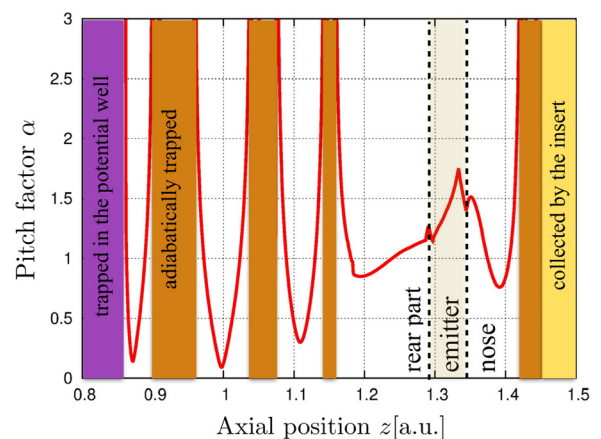


FIG. 10. The pitch factor at the cavity versus the axial position of the emitting point of the first industrial prototype of the EU 170 GHz/2 MW coaxial cavity gyrotron project for ITER.

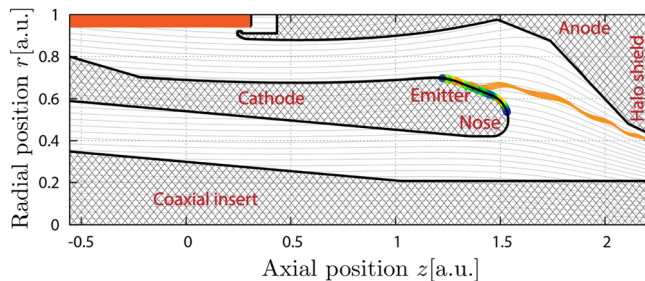


FIG. 11. Electron trappings in the refurbished first industrial prototype of the EU 170 GHz/2 MW coaxial cavity gyrotron project for ITER.

magnitude lower. By modifying the magnetic field configuration, it was possible to form a magnetic potential well in the region between the inner side of the cathode and the coaxial insert that coincided with a dramatic decrease of the voltage stand-off.

Later on, the first tests with the industrial tube validated the cold test results of the mock-up device with respect to high voltage performance. Furthermore, no major problem was observed in short-pulse operation (1 ms) of the gyrotron and the goal of 2 MW of generated power was reached shortly after the beginning of the experiments.²⁷ However, a body current of few of mA was measured during operation as well as a disagreement between theoretical and experimental results on the starting current of the modes was observed without influencing the gyrotron nominal operation.

Both observations could be related to the existence of adiabatically trapped electrons. Due to the fact that the pitch factor of the electrons emitted from the rear part of the cathode is quite high, secondary electrons contribute to the accumulation of adiabatically trapped electrons on the magnetic field lines which pass through this area. These magnetic field lines are in a very close vicinity to the part of the anode which is called halo shield (see Fig. 11).²³ As a result, a part of the adiabatically trapped electrons is collected by the halo shield and a body current is measured. Concerning the high starting currents of the modes at the cavity, several hypotheses have been studied in order to explain the disagreement between the theoretical and the experimental results without success, such as a possible misalignment of the tube to the magnetic field.²⁸

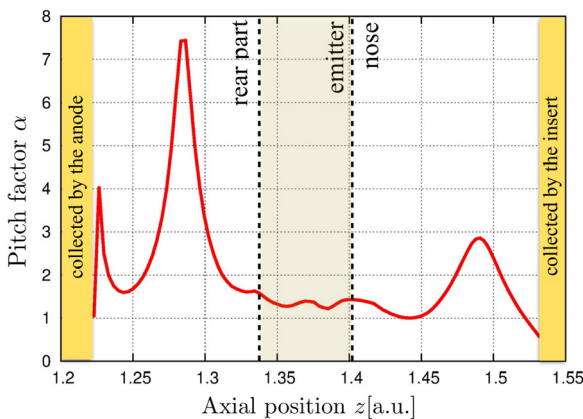


FIG. 12. The pitch factor at the cavity versus the axial position of the emitting point of the refurbished first industrial prototype of the EU 170 GHz/2 MW coaxial cavity gyrotron project for ITER.

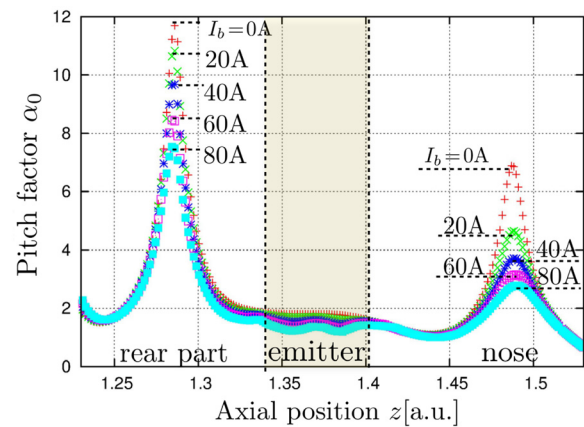


FIG. 13. Pitch factor α_0 versus the axial position of the emitting point for several values of the beam current I_b .

However, a hypothesis related to the influence of the adiabatically trapped electrons seems to be consistent with that behaviour. The influence of the beam current I_b on the pitch factor at the cavity of the electrons emitted from the cathode surfaces is shown in Fig. 13. For low currents, the pitch factor of the electrons emitted from the rear part and the nose of the cathode gradually increases to 12 and to around 7, respectively. These values are much higher than the threshold $\alpha_{\max} \approx 3$ of this gyrotron, and therefore a very large number of secondary electron will be accumulated in the adiabatic traps initiated from the rear part and the cathode nose, influencing in this way the beam quality and the interaction at the cavity. Therefore, the influence of the trapped electrons at low beam currents could be a possible reason for the high starting currents of the cavity modes.

The electron trapping mechanisms were more recently tested on a third geometry:²⁵ the short-pulse prototype of the EU 170 GHz/1 MW cylindrical cavity gyrotron project for ITER.²⁶ Using the flexibility of the superconducting magnet at KIT, it was possible to characterize the gyrotron behavior with three different magnetic profiles, for which the beam parameters at the cavity were very similar, while the status of the MIG concerning electron trapping is quite different as shown in Figs. 14 and 15. In case A, a potential well formed at the rear part while a maximum pitch angle of the order of 2.4 is calculated for the electrons emitted from the cathode nose. In case B, no potential well is formed and the maximum pitch factor of the electrons emitted from the cathode nose is slightly higher than 3. Finally, in case C, the geometry is free of a potential well but the pitch factor at the cavity of the electrons emitted from the cathode nose is more than 4 which is much higher value than the limit $\alpha_{\max} \approx 3$ for accelerating voltage $U_a = 78$ kV and magnetic compression $\kappa_b \approx 32$.

The voltage stand-off of the three cases was tested using a high impedance power supply and cold emitter. In cases B and C, the voltage stand-off was excellent, while it was poor and unstable in case A, demonstrating the negative influence of potential well. Later-on experiments in short-pulses with a hot emitter were performed. According to the electrostatic electron beam simulations, the beam parameters at the cavity are very similar in the three cases, and close performances would be expected. However, it appeared that the high

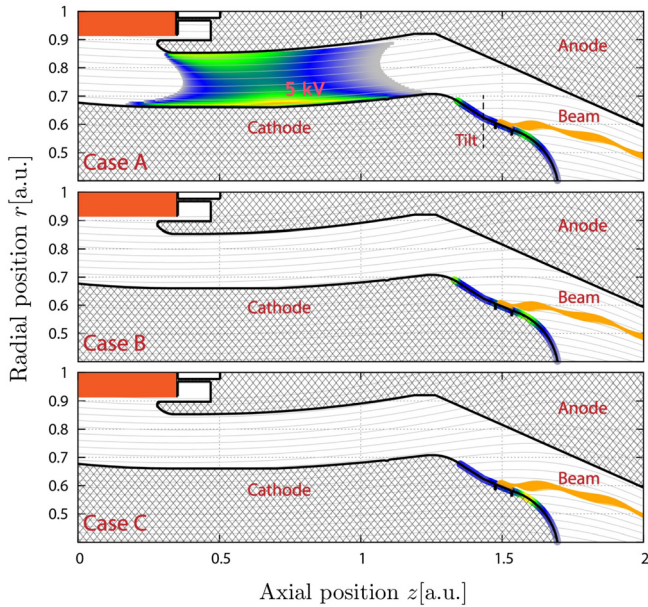


FIG. 14. Electron trapping in three operating points of the short-pulse prototype of the EU 170 GHz/1 MW cylindrical cavity gyrotron project for ITER.

values of the pitch factor at the cavity for the electrons emitted from the cathode nose could play an important role in the operation. In particular, a power in excess of 1 MW and electronic efficiency of 34% were measured in cases A and B in pulse lengths of 1 ms. As expected, the potential well does not have any influence on the gyrotron operation in such a time scale. In case C, in which the pitch factor is higher than the safe value, it was not possible to excite the nominal mode for voltages higher than 72 kV. At this voltage, the generated rf power was limited to 600 kW. Additionally, low-frequency parasitic oscillations were detected, and the stray radiation level was doubled in comparison to cases A and B.

V. DESIGN PRINCIPLES

The shape of the MIG electrodes and the magnetic field lines play an important role in the suppression of electron trapping mechanisms. Following the discussion of Sections

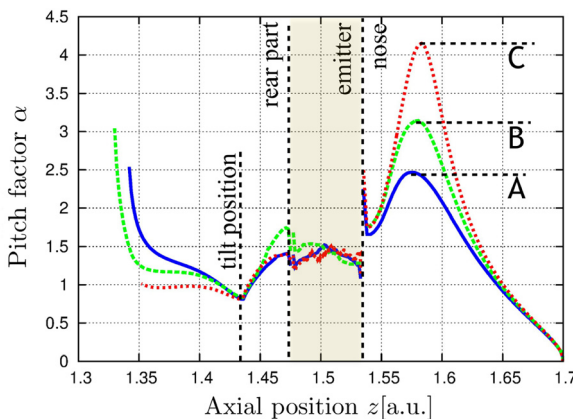


FIG. 15. Comparison of the pitch factor at the cavity versus the axial position of the emission point for the three operating points of the short-pulse prototype of the EU 170 GHz/1 MW conventional cavity gyrotron project.

II–IV, some very general and empirical design principles are discussed in order (i) to keep the pitch factor of the electrons emitted from the cathode surface below the threshold for reflections and (ii) to avoid the formation of magnetic potential wells.

A general rule to keep the pitch factor at the cavity of the electrons emitted from the cathode surface at a low level is to minimise the initial transverse velocity of the electrons at the cathode¹⁰ defined as $v_0 = E \times B / B^2$. This could happen in two ways: (i) keeping the electric field E as small as possible and/or (ii) designing the cathode surfaces at a high angle with respect to the magnetic field lines in order to minimize the angle between the electric and the magnetic field vectors. However, the pitch angle of the electrons emitted from all parts of the cathode should always be checked using numerical tools, due to the non-adiabaticity in the gun region.

Introducing a tilt at the rear part of the cathode could significantly decrease the pitch factor of the electrons emitted from this area as shown in Fig. 14. A decrease of the trapped charge in the presence of the tilt at the cathode rear part was also demonstrated using PIC simulations for a low power gyrotron.²⁹ The advantages of this tilt are as follows: (i) the local electric field around the tilt decreases and (ii) the angle between the vectors of the electric and magnetic field also decreases. On the other hand, the use of higher angles for the emitter ring and a longer cathode nose facilitates to keep the pitch factor values low for the secondary electrons emitted from the nose. However, this is not always possible. Such an example is the coaxial cavity diode design in which the radial thickness of the cathode is small due to the presence of the coaxial insert, as shown in Figs. 9 and 11. In order to address this issue, alternative configurations are under investigation, such as the inverse gun³⁰ for the 170 GHz/2 MW coaxial cavity gyrotron at KIT³¹ and a triode gun³² for the design of a 238 GHz/2 MW coaxial cavity gyrotron for DEMO.

Concerning the second electron trapping mechanism, in order to avoid the formation of a potential well in the regions where the electric field has a significant value, the following two general design principles should be considered: (i) The cathode electrode should not intersect the same magnetic field line twice. (ii) No magnetic field line should approach very close an anode surface from two sides without intersecting it. These principles, although a good starting point, are not always sufficient to avoid the formation of a potential well, especially in complex geometries. It is thus safer to use a numerical tool which identifies accurately the place, the size, and the depth of the potential wells formulated in the MIG region, to verify the design.

VI. CONCLUSIONS

The presence of trapped electrons in the MIG region can cause many problems to the gyrotron operation such as decreased efficiency, failure of the excitation of the nominal operating mode at the cavity, voltage stand-off instabilities, parasitic oscillations, and increased stray radiation level. Several issues related to the two types of electron trapping

mechanisms which can take place in gyrotrons were discussed. Two MIG design criteria were proposed for the suppression of electron trapping in order to minimize the risk of possible problems. The major advantage of the proposed design criteria is that checking whether a design satisfies them or not is an easy and quick process requiring just a self-consistent electrostatic trajectory simulation code. The importance of the design criteria was also demonstrated by comparison and analysis of the experimental results of three different high power gyrotron tubes. Finally, several empirical design principles were presented for the satisfaction of both criteria.

ACKNOWLEDGMENTS

This work was supported by Fusion for Energy under Contract Nos. F4E-GRT-008, F4E-GRT-034, F4E-GRT-049, F4E-GRT-432, and F4E-GRT-553 to the European Gyrotron Consortium (EGYC). EGYC is a collaboration among CRPP, Switzerland; KIT, Germany; HELLAS, Greece; and IFP-CNR, Italy. The views expressed in this publication do not necessarily reflect the views of F4E or the European Commission.

The authors would like to warmly thank Dr. S. Alberti, Dr. S. Kern, and Professor I. L. Vomvoridis for fruitful discussions, V. Rumko for help to design the figures, Dr. E. Borie for her contribution to the text quality of the manuscript, as well as the EGYC teams performing the experiments of the two industrial prototypes for the EU 170 GHz/1 MW coaxial cavity gyrotron project for ITER which took place at CRPP in Lausanne and the short pulse prototype of the EU 170 GHz/1 MW cylindrical cavity gyrotron project for ITER which took place at KIT in Karlsruhe. Part of the simulations was performed at HELIOS super computer system at IFERC, Japan.

¹I. Gr. Pagonakis and J. L. Vomvoridis, "The self-consistent 3D trajectory electrostatic code Ariadne for gyrotron beam tunnel simulation," in *Joint 29th International Conference on Infrared and Millimeter Waves IRMMW and 12th International Conference on Terahertz Electronics*, Karlsruhe, Germany, 27 September-1 October (2004), p. 657.

²S. Illy, J. Zhang, and J. Jelonnek, "Gyrotron electron gun and collector simulation with the ESRAY beam optics code," in *16th International Vacuum Electronics Conference (IVEC)*, Beijing, China, 27–29 April (2015), P1.1.

³T. M. Tran, D. R. Whaley, S. Merazzi, and R. Gruber, "DAPHNE, a 2D axisymmetric electron gun simulation code," in *6th Joint EPS-APS International Conference on Physics Computing*, Lugano, Switzerland, 22–26 August (1994), p. 491.

⁴W. B. Herrmannsfeldt, "EGUN—An electron optics and gun design program," in SLAC, Stanford, California (1988).

⁵B. Piosczyk, G. Dammertz, O. Dumbrajs, M. V. Kertikeyan, M. K. Thumm, and X. Yang, "165-GHz coaxial cavity gyrotron," *IEEE Trans. Plasma Sci.* **32**, 853 (2004).

⁶J. P. Hogge, T. P. Goodman, S. Alberti, F. Albajar, K. A. Avramides, P. Benin, S. Bethuys, W. Bin, T. Bonicelli, A. Bruschi, S. Cirant, E. Droz, O. Dumbrajs, D. Fasel, F. Gandini, G. Ganenbein, S. Illy, S. Jawla, J. Jin, S. Kern, P. Lavanchy, C. Lievin, B. Marletaz, P. Marmillod, A. Perez, B. Piosczyk, I. Pagonakis, L. Porte, T. Rzesnicki, U. Siravo, M. Thumm, and M. Q. Tran, "First experimental results from the European Union 2-MW coaxial cavity ITER prototype," *Fusion Sci. Technol.* **55**, 204 (2009).

⁷S. Cauffman, M. Blank, Ph. Borchard, and K. Felch, "Overview of fusion gyrotron development programs at 110 GHz, 117.5 GHz, 140 GHz, and 170 GHz," in *38th International Conference on Infrared, Millimeter and Terahertz Waves (IRMMW-THz)*, Mainz on the Rhine, Germany, 1–6 September (2013), Mo 1-1.

⁸R. Pu, G. S. Nusinovich, O. V. Sinitsyn, and T. M. Antonsen, Jr., "Effect of the thickness of electron beams on the gyrotron efficiency," *Phys. Plasmas* **17**, 83105 (2010).

⁹A. Schlaich, C. Wu, I. Gr. Pagonakis, K. Avramides, S. Illy, G. Ganenbein, J. Jelonnek, and M. Thumm, "Frequency-based investigation of charge neutralization processes and thermal cavity expansion in gyrotrons," *J. Infrared Millim. THz Waves* **36**, 797 (2015).

¹⁰Sh. E. Tsimring, *Electron Beams and Microwave Vacuum Electronics* (John Wiley & Sons, Inc., Hoboken, New Jersey, 2007).

¹¹O. I. Louksha, G. G. Sominski, and D. V. Kas'yanenko, "Experimental study and numerical simulation of electron beam in gyrotron-type electron-optical system," in *Proceedings of International University Conference on "Electronics and Radiophysics of Ultra-High Frequencies"*, St. Petersburg, Russia, 24–28 May (1999), p. 130.

¹²V. N. Manuilov, "Numerical simulation of low-frequency oscillations of the space charge and potential in the electron-optical system of a gyrotron," *Radiophys. Quantum Electron.* **49**, 786 (2006).

¹³A. N. Kuftin, V. K. Lygin, V. N. Manuilov, B. V. Raisky, E. A. Soljanova, and Sh. E. Tsimring, "Theory of helical electron beams in gyrotrons," *Int. J. Infrared Millim. THz Waves* **14**, 783 (1993).

¹⁴Sh. E. Tsimring and V. E. Zapevalov, "Experimental study of intense helical electron beams with trapped electrons," *Int. J. Electron.* **81**, 199 (1996).

¹⁵V. N. Manuilov and S. A. Polushkin, "Behavior of helical electron beams in gyrotrons with high pitch factors," *Radiophys. Quantum Electron.* **52**, 714 (2009).

¹⁶M. A. Furman and M. T. F. Pivi, "Probabilistic model for the simulation of secondary electron emission," *Phys. Rev. ST Accel. Beams* **5**, 124404 (2002).

¹⁷A. Shih and C. Hor, "Secondary emission properties as a function of the electron incidence angle," *IEEE Trans. Electron Devices* **40**, 824–829 (1993).

¹⁸G. A. Harrower, "Energy spectra of secondary electrons from Mo and W for low primary energies," *Phys. Rev.* **104**, 52 (1956).

¹⁹H. Bruining, *Physics and Applications of Secondary Electron Emission* (Pergamon Press, McGraw-Hill Book Co., New York, 1954).

²⁰B. Piosczyk, C. Iatrou, G. Dammertz, and M. Thumm, "Single-stage depressed collectors for gyrotrons," *IEEE Trans. Plasma Sci.* **24**, 579 (1996).

²¹K. Sakamoto, M. Tsuneoka, A. Kasugai, T. Imai, T. Kariya, K. Hayashi, and Y. Mitsunaka, "Major improvement of gyrotron efficiency with beam energy recovery," *Phys. Rev. Lett.* **73**, 3532 (1994).

²²Y. Itikawa, "Cross sections for electron collisions with nitrogen molecules," *J. Phys. Chem. Ref. Data* **35**, 31 (2006).

²³I. Gr. Pagonakis, J.-P. Hogge, T. Goodman, S. Alberti, B. Piosczyk, S. Illy, T. Rzesnicki, S. Kern, and C. Lievin, "Gun design criteria for the refurbishment of the first prototype of the EU 170 GHz/2 MW/CW coaxial cavity gyrotron for ITER," in *34th International Conference on Infrared, Millimeter and Terahertz Wave (IRMMW-THz)*, Busan, Korea, 21–25 September (2009).

²⁴I. Gr. Pagonakis, J.-P. Hogge, S. Alberti, S. Illy, B. Piosczyk, S. Kern, C. Lievin, and M. Q. Tran, "Status of the EU 170 GHz/2 MW/CW coaxial cavity gyrotron for ITER: The dummy gun experiment," in *35th International Conference on Infrared, Millimeter, and Terahertz Waves (IRMMW-THz)*, Rome, Italy, 5–10 September (2010).

²⁵T. Rzesnicki, I. Gr. Pagonakis, A. Samartsev, K. Avramides, G. Ganenbein, S. Illy, J. Jelonnek, J. Jin, C. Lechte, M. Losert, B. Piosczyk, M. Thumm, and EGYC Team, "Recent experimental results of the European 1 MW, 170 GHz short-pulse gyrotron prototype for ITER," in *40th International Conference on Infrared, Millimeter, and Terahertz Waves (IRMMW-THz)*, Hong Kong, China, 23–28 August (2015).

²⁶I. Gr. Pagonakis, F. Albajar, S. Alberti, K. Avramides, T. Bonicelli, F. Braunmueller, A. Bruschi, I. Chelis, F. Cismondi, G. Ganenbein, V. Hermann, K. Hesch, J.-P. Hogge, J. Jelonnek, J. Jin, S. Illy, Z. Ioannidis, T. Kobarg, G. Latsas, F. Legrand, M. Lontano, B. Piosczyk, Y. Rozier, T. Rzesnicki, C. Schlatter, M. Thumm, I. Tigelis, M. Q. Tran, T.-M. Tran, J. Weggen, and J. L. Vomvoridis, "Status of the development of the EU 170 GHz/1 MW/CW gyrotron," *Fusion Eng. Des.* **96–97**, 149–154 (2015).

²⁷S. Kern, J.-P. Hogge, S. Alberti, K. Avramides, G. Ganenbein, S. Illy, J. Jelonnek, J. Jin, F. Li, I. Gr. Pagonakis, B. Piosczyk, T. Rzesnicki, M. K. Thumm, I. Tigelis, M. Q. Tran, and the Whole EU Home Team at EGYC, "Experimental results and recent developments on the EU 2 MW 170 GHz

- coaxial cavity gyrotron for ITER,” in 17th Joint Workshop on Electron Cyclotron Emission and Electron Cyclotron Resonance Heating, Deurne, The Netherlands, 7–11 May (2012).
- ²⁸K. A. Avramidis, I. Gr. Pagonakis, Z. C. Ioannidis, and I. G. Tigelis, “Numerical investigations on the effects of electron beam misalignment on beam-wave interaction in a high-power coaxial gyrotron,” in 38th International Conference on Infrared, Millimeter, and Terahertz Waves (IRMMW-THz), Mainz, Germany, 14–19 September (2013).
- ²⁹M. Yu. Glyavin, A. D. Kuntsevich, and V. N. Manuilov, “Suppression of the oscillatory modes of a space charge in the magnetron injection guns of technological gyrotrons,” *J. Infrared Millim. THz Waves* **36**, 7 (2015).
- ³⁰S. Ruess, I. Gr. Pagonakis, T. Rzesnicki, G. Gantenbein, S. Illy, M. Thumm, and J. Jelonnek, “A design proposal for an optimized inverse magnetron injection gun for the KIT 2 MW/170 GHz modular coaxial cavity gyrotron,” in *16th International Vacuum Electronics Conference (IVEC)*, Beijing, China, 27–29 April (2015), S4.1.
- ³¹T. Rzesnicki, G. Gantenbein, J. Jelonnek, J. Jin, I. Gr. Pagonakis, B. Piosczyk, A. Samartsev, A. Schlaich, and M. Thumm, “2 MW, 170 GHz coaxial-cavity short-pulse gyrotron—Single stage depressed collector operation,” in *39th International Conference on Infrared, Millimeter and THz Waves (IRMMW-THz)*, Tucson, AZ, USA, 14–19 September (2014), W4/D5.
- ³²J. Franck, I. Gr. Pagonakis, K. A. Avramidis, G. Gantenbein, S. Illy, M. Thumm, and J. Jelonnek, “Magnetron injection gun for a 238 GHz 2 MW coaxial-cavity gyrotron,” in *9th German Microwave Conference (GeMiC)*, Nürnberg, Germany, 16–18 March (2015), p. 260.